Research Square

Preprints are preliminary reports that have not undergone peer review.
They should not be considered conclusive, used to inform clinical practice,
or referenced by the media as validated information.

Forest water-use strategies at high-latitude and -altitude regions over the last Millennium

Olga Churakova (Sidorova)

olga.churakova@wsl.ch

Swiss Federal Institute for Forest, Snow and Landscape Research WSL, Siberian Federal University, Krasnoyarsk, Russian Federation https://orcid.org/0000-0002-1687-1201

Mikhail Zharkov

Rolf Siegwolf

Swiss Federal Research institute for Forest Snow and Landscape, WSL https://orcid.org/0000-0002-0249-0651

Matthias Saurer

Swiss Federal Institute for Forest Snow and Landscape Research WSL https://orcid.org/0000-0002-3954-3534

Article

Keywords: δ13C in tree-ring cellulose; ci/ca, iWUE, conifers, subarctic, Asia, the Alps, climate

Posted Date: June 10th, 2026

DOI: https://doi.org/10.21203/rs.3.rs-9661662/v1

License: This work is licensed under a Creative Commons Attribution 4.0 International License.
Read Full License

Additional Declarations: There is **NO** Competing Interest.

Forest water-use strategies at high-latitude and -altitude regions over the last Millennium

Running title: MILLENNIAL FOREST WATER-USE

Olga V. Churakova (Sidorova)[1,2], Mikhail Zharkov[2], Rolf Siegwolf[1], Matthias Saurer[1]

[1]Swiss Federal Institute for Forest, Snow and Landscape Research WSL, Switzerland

[2]Siberian Federal University, Krasnoyarsk, Russian Federation

Contact information: Olga Churakova olga.churakova@wsl.ch; ORCID https://orcid.org/0000-0002-1687-1201

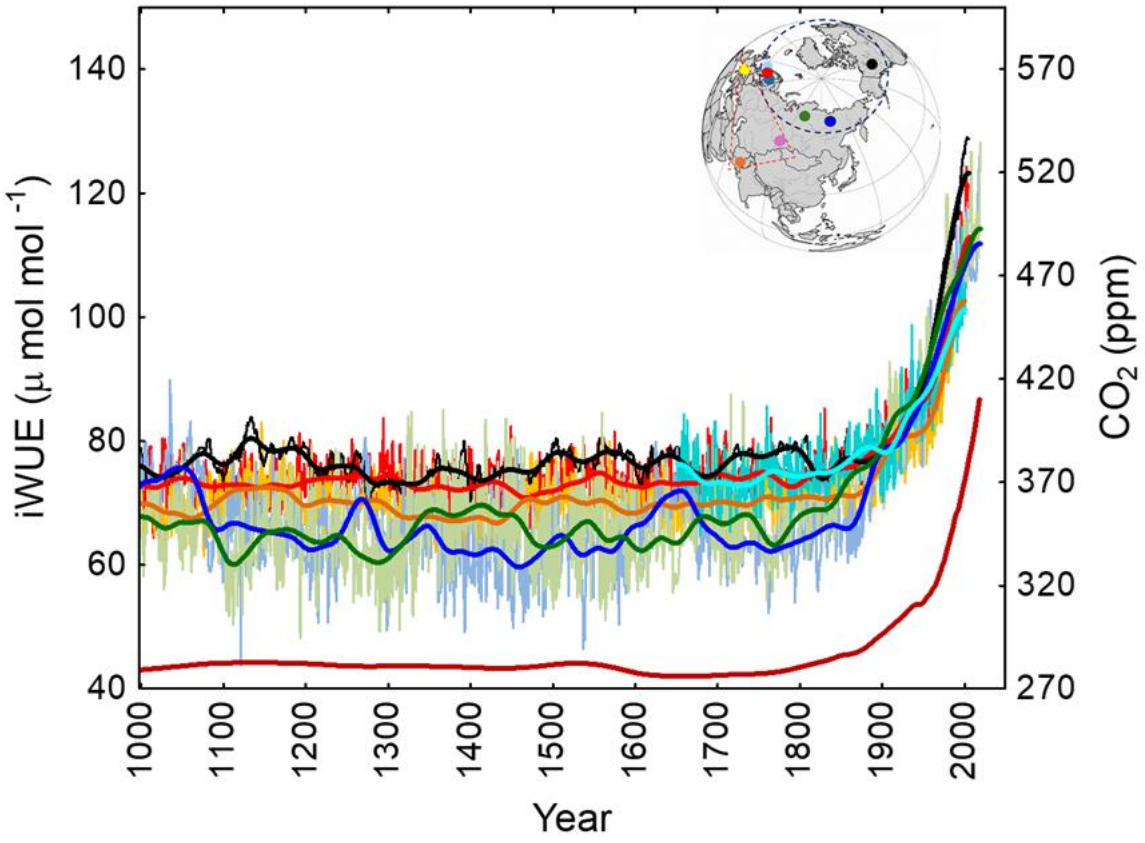
Abstract

We present annually resolved millennial $\delta^{13}C$ tree-ring cellulose chronologies from 6 regions covering northeastern and eastern Russia, western Canada, Sweden, Norway, and Finland, and 3 regions from the Swiss Alps and Inner and Central Asia. We evaluated iWUE responses of conifer forests to changes in CO_2 and climate during pre-industrial (CE 1000-1899) and anthropogenically influenced (CE 1900-1989) periods.

Our results show that after moderate iWUE variations throughout most of the record, a major increase occurred in the 20th century. During the industrial period, iWUE increased across the HL gradient from west (15.7 %) to east (33.0 %), while along high-elevated sites range 13.3 - 25.1 %. The most pronounced increase was observed at the most continental sites in Siberia and in the Altai mountains. We revealed that iWUE and related eco-physiological processes over the strongly human-influenced 20th century were primarily modulated by changes in atmospheric CO_2 concentration, although this effect has diminished in the last decades. In contrast, climate change dominated changes in iWUE in the pre-industrial period. The industrial iWUE increase is unprecedented for HL and HA over the past millennium. However, since the 2000s, Siberian forests demonstrate significant resilience to increased human-induced CO_2, associated with stable iWUE.

Keywords (6-10): $\delta^{13}C$ in tree-ring cellulose; c_i/c_a, iWUE, conifers, subarctic, Asia, the Alps, climate

Graphical Abstract:



Highlights:

- The 3rd millennium iWUE values are higher at HL but show reduction towards 2020s due to CO_2 emissions.
- An increase in iWUE is revealed from west to east across the subarctic and from High- to Inner Asia.
- Pre-industrial (CE 1000-1899) forest iWUE patterns are modulated by climate

Introduction

Forest ecosystems from high-latitude (HL) and high-altitude (HA) regions of the Northern Hemisphere (NH) are valuable indicators of environmental changes and areas for dendrochronological, biogeochemical, and eco-physiological studies because trees growing there are particularly sensitive to changes in temperature, moisture deficit and nutrients (Vaganov et al., 2006; Sidorova et al., 2008, 2010, 2012; Körner et al., 2012). Trees from these regions are also long-lived and dead trunks sometimes preserved, making them ideal archives of environmental conditions and their impact on tree growth over long time spans.

In Arctic and Alpine regions, climate change is progressing much faster than on global average (Druckenmiller et al., 2025). The increase in air temperature and reduction of precipitation results in thawing of permafrost, which covers a quarter of the NH land surface and contains twice the amount of carbon that is currently present in the atmosphere (Bowden 2010). As temperature increases, vapor pressure deficit will likely increase in subarctic ecosystems resulting in increased evapotranspiration, which impact, in particular, water relations in trees (Cable et al., 2013; Churakova et al. et al., 2020, 2024). The potential effects of increased evaporative demand, forest water-use under permafrost thaw and frequent drought waves are leading to wildfires worldwide.

These climate changes along with the carbon dioxide increase in the atmosphere have direct impacts on tree physiology (e.g., photosynthesis). Other greenhouse gases (GHSs), have an indirect impact via climatic parameters, such as increased temperature, enhanced vapor pressure deficit and reduction of precipitation over the past decades. Permafrost thawing causes an enhanced emission of CH_4 and N_2O into the atmosphere (MacFarling et al., 2006; Lan 2025; Belmecheri and Lavergne, 2020, **Fig. S1**), further accelerating temperature increase. Atmospheric carbon dioxide (CO_2) is one of the most important greenhouse gases because of its long residence time in the atmosphere (IPCC, 2007). On one hand, the increasing atmospheric CO_2 accumulation results in an increasing global mean air temperature (IPCC, 2007), on the other hand, it affects directly the eco-physiology of plants. Many impacts of global climate change are already apparent in the subarctic including: (i) spatially complex

patterns of reduced and increased rates of tree growth (Briffa 1998; Lloyd & Bunn 2007); (ii) larger and more extensive fires and insect outbreaks (Soja et al. 2007); and (iii) a range of effects due to permafrost degradation, including new wetland development (thermokarst lakes) and collapsing of the ground surface (Biskaborn et al., 2019; Turetsky 2019; Zandt et al., 2020) with the associated loss of trees.

The water cycle is a complex target at the HL and HA and, therefore, its long-term changes not well understood. Both, temperature and moisture signals, like vapor pressure deficit (VPD) and soil water availability are well captured by stable carbon isotopes and their analysis is, therefore, useful for assessing tree responses to changes of the water cycle. The stable carbon isotope ratio $^{13}C/^{12}C$ is related to the ratio of photosynthesis (A) to stomatal conductance (g), which is defined as carbon gain per molecular water loss determining the intrinsic water-use efficiency (iWUE) (Dawson and Siegwolf 2007, Saurer and Voelker 2022). This is an important eco-physiological property, particularly for plants growing in dry areas, and may determine which plants are better adapted to enhanced warming. Plants with high iWUE tend to close stomata fast under dry conditions and, therefore, are less prone to hydraulic failure (McDowell et al., 2008; Saurer et al., 2014). Because transpiration is influenced by the stomatal conductance (g) and vapor pressure deficit (VPD), the iWUE also depends on the evaporative demand (Saurer et al., 2014). VPD is a crucial parameter impacting photosynthesis via stomatal conductance. Temperature increase causes an enhancement in VPD, and soil moisture decreases through evapotranspiration (Williams et al., 2013). A few recent studies showed a significant effect of the global increased VPD changes (Zhang et al., 2019) such as reduction in vegetation growth and forest mortality (McDowell et al., 2008; Yuan et al., 2019).

So far, iWUE trends were analysed mainly over the 20th century across northern subarctic (Saurer et al., 2004; Churakova (Sidorova) et al., 2016, 2020), Europe (Saurer et al., 2014; Frank et al., 2015; Churakova (Sidorova) et al., 2016) using annually resolved stable carbon isotope chronologies. Saurer et al. (2014) showed a spatial variability, and temporal trends of water use efficiency of European forests by demonstrating south-to-north gradient, as well as a general increase in iWUE during the

20th century, which was interpreted as the result of a combined effect: increased CO_2, increased temperature, and decreased precipitation leading to soil moisture deficit.

Globally, tree-ring chronologies representing 34 species across 10 biomes have shown that a ~40% increase in tree iWUE since 1901 coincide with a ~34% increase in atmospheric CO_2 (c_a), although mean iWUE, and the rates of increase, varied across biomes (Mathias and Thomas 2021). Based on synthesized 422 tree-ring isotope series from angiosperms and gymnosperms Adams et al. (2020) and Zhang et al. (2026) concluded that increased iWUE does not stimulate tree productivity over the recent decades 1851-2015. However, to our knowledge there are not yet any studies on revealing and understanding water-use changes by conifer trees from the HL and HA regions over the last millennium.

In this study we aim to: (i) reconstruct iWUE based on millennial annually resolved $\delta^{13}C$ in tree-ring cellulose chronologies from HL and HA regions; (ii) reveal impact of CO_2 and climatic variables like air temperature, precipitation, relative humidity and vapor pressure deficit, and cloud cover on iWUE changes over the pre-industrial (CE 1000-1899) and industrial (since 1900s) periods; and (iii) evaluate how water-use changes by conifer forests developed over the past millennia can be used to estimate potential future changes for the direct CO_2 versus the indirect, climatic impact.

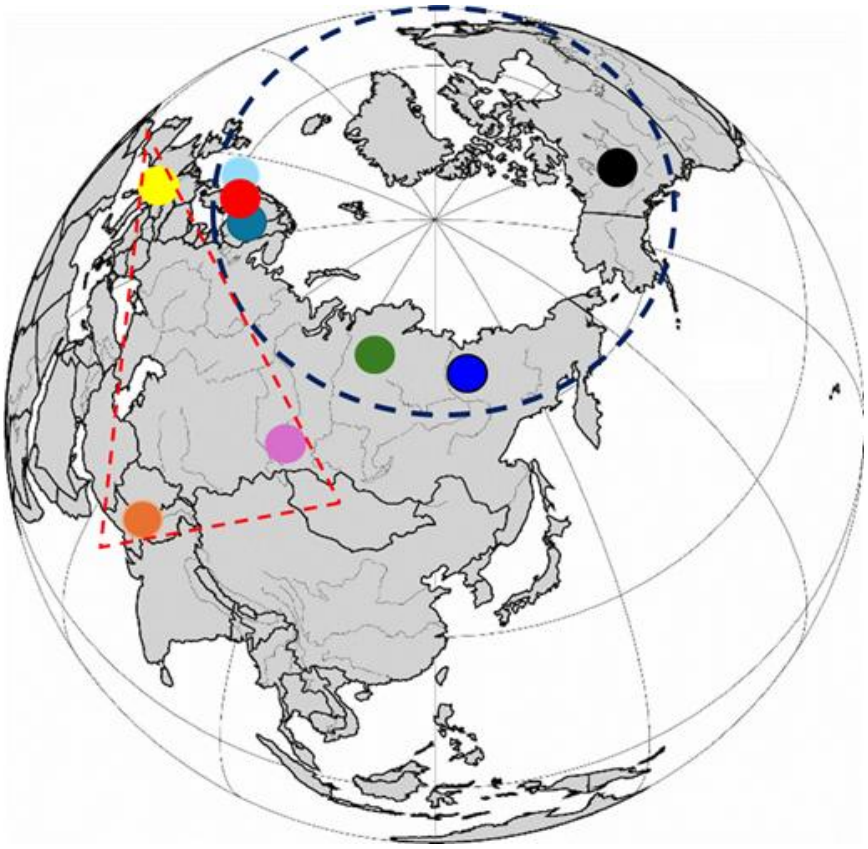
2 Methods and Materials

2.1 Study regions

We selected regions at high-latitudes (HL, above 60° N) and high-altitudes (HA, above 2100 m asl,) in the NH, which are highly sensitive to climate change, and for which annually resolved stable carbon ($\delta^{13}C$) isotope chronologies are available over the past millennia (**Table 1**).

The main tree species across the subarctic circle are represented by *Larix* in the Siberian subarctic (TAY, YAK)*, Pinus* in Fennoscandia (NOR, SWE, FIN) and *Picea glauca* in CAN. At the high elevations *Larix* in ALT and LOT, and *Juniperus turkestanica* in PAK are dominant tree species.

(a)



(b)

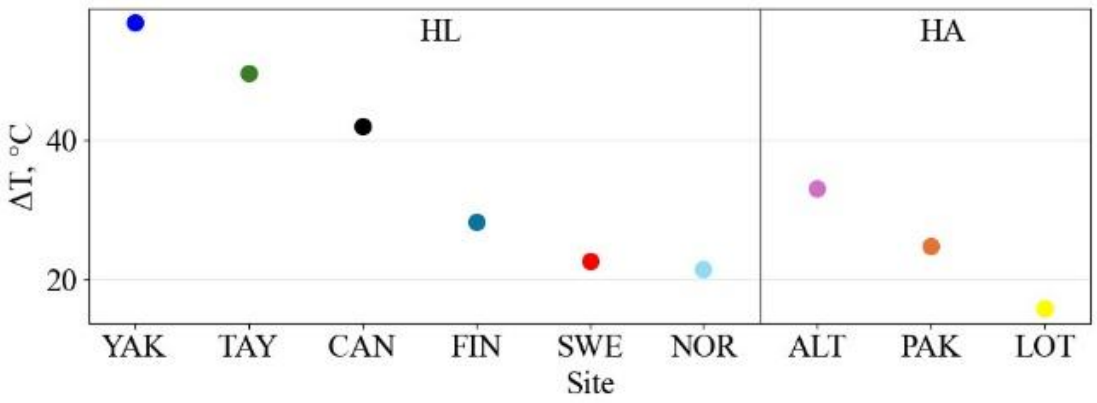


Figure 1. Location of study sites at the high-latitudes (HL, subarctic circle) with millennial $\delta^{13}C$ chronologies obtained for: Russian Federation (northeastern Yakutia, YAK, blue circle and eastern Taimyr TAY - green circle), Quebec-Labrador Peninsula (Canada, CAN - black circle); Laanila (Finland, FIN - turquoise circle); Torneträsk (Sweden, SWE - red circle) and Forfjörd (Norway, NOR - turquoise circle). The high-altitude sites (HA, red dotted triangle) are represented by: Mongun Taiga

(Russian Altai, ALT - pink circle); Karakorum, Moor (Pakistan, PAK - yellow circle) and Loetschental (Switzerland, LOT - orange circle) **(a)**. Sites are represented in order of the continentality, describing the difference between maximum and minimum monthly air temperature over the past century for each study site (**b, Table 1**).

Table 1. Study site and tree characteristics of millennial $\delta^{13}C$ in tree-ring cellulose chronologies at **(a)** high-latitude (HL) and **(b)** high-altitude (HA) regions.

Site name	Site code	Site coordinates asl	Period, Common Era (CE)	Tree species	Climate variables	References
		(a) High-latitude sites (HL)				
North-eastern Yakutia, Russian Federation	YAK	69° N, 149° E 250-300 m asl	516-2021	*Larix cajanderi* Mayr.	- July temperature - July precipitation - July vapor pressure deficit - July sunshine duration	Churakova (Sidorova) et al. 2020, 2023
Taimyr Peninsula, Russian Federation	TAY	68° N, 103° E 200-300 m asl	516-2020	*Larix gmelinii* Rupr. Rupr.	- July precipitation	Churakova (Sidorova) et al. 2021, 2023 https://zenodo.org/records/5426606
Quebec-Labrador Peninsula, Canada	CAN	69° N, 135°W	997–2006	*Picea glauca* (Moench) Voss	- June temperature	Gennaretti et al. 2017
Laanila, Finland	FIN	68° N 27° E 230 m asl	1640-2002	*Pinus sylvestris L.*	- July-August cloud cover - June-August temperature	Gagen et al. 2011
Torneträsk, Sweden	SWE	68° N, 18° E 350-450 m asl	800-2009	*Pinus sylvestris* L.	- June-August sunshine - July-August temperature	Loader et al. 2013
Forfjord, Norway	NOR	68° N, 15° E	990-2001	*Pinus sylvestris* L.	- June-August temperature	Young et al. 2019
		(b) High-altitude sites (HA)				
Altai-Sayan Mountain Range region Mongun Taiga	ALT	51°N, 89°E 2300 m asl	516-2016	*Larix sibirica* Ledeb.	- July temperature - July sunshine duration	Churakova-Sidorova 2022 https://zenodo.org/records/6467290
Moor, Karakorum, Pakistan	PAK	36°N, 76°E 2900-3700 m asl	828-2000	*Juniperus excels*	- July temperature	Treydte et al., 2006
Loetschental, Switzerland	LOT	46°N, 7°E 2100-2200 m asl	1650-2004	*Larix decidua* Mill.	- July-August temperature	Kress et al., 2010

2.2 Climate data

Gridded climate data were computed for averaged summer June-July-August (JJA) air temperature (Temp), potential evapotranspiration (Evp), and mean summer relative humidity for the common period from CE 1901 to 2024 with the grid net resolution 0.5°. Data were downloaded from https://climexp.knmi.nl (accessed April 2026) (**Table S1, Fig. 4**).

Our earlier study showed that gridded precipitation data poorly agree with the local weather stations for remote regions like Khatanga (TAY) and Chokurdach (YAK) (Zharkov et al., 2021). Therefore, for both Siberian regions, the local precipitation (Prec) data http://aisori-m.meteo.ru/aisori-m/result.xhtml (accessed April 2026) for the period from 1950 to 2024 were used. Vapor pressure deficit (VPD) was calculated for YAK and TAY based on the local weather station data by applying Buck's (1981).

Gridded CRU TS 4.09 precipitation (Prec) and vapor pressure deficit (VPD) data for western Europe (Fennoscandia) and Canada regions were used (**Table S1**). The CRU TS4.09 average summer JJA air temperature at HL from CE 1901 to 2024 ranges between +6.8°C in the Siberian subarctic to + 11.6°C in the Canadian subarctic (**Table S1**). Summer Evp is twice as high in Canada (0.6 kPa) compared to YAK (0.3kPa). VPD summer values in SWE and TAY are also lower (0.34 and 0.37 kPa), respectively than in CAN. Total sum of summer precipitation increases from northeastern part of subarctic from YAK (35mm), Taimyr (45.8 mm) and Canada (41.5 mm) to western part of Fennoscandia (228 mm) from CE 1950 to 2021. The LOT site in the Swiss Alps shows higher amount of summer precipitation (465 mm) compared to PAK (61 mm).

The heat maps between iWUE for both HL and HA versus climatic parameters were generated using Seaborn, Python package for data visualization (Waskom, 2021).

2.3 Computing of intrinsic Water-Use Efficiency (iWUE)

148 The intrinsic water-use efficiency (iWUE) was computed based on the $\delta^{13}C$ in tree-ring cellulose (raw
149 data, e.g., uncorrected for $\delta^{13}C$ atmospheric CO_2 concentration due to fossil fuel combustion) for both
150 HL and HA sites, which is defined as follows:

151 $$iWUE = (c_a - c_i)/1.6 \quad \text{(Eq. 1)}$$

152 $$c_i = c_a \bullet ((\delta^{13}C_a - \delta^{13}C_{trc} - a)/(b - a)) \quad \text{(Eq. 2)}$$

153 *a*—is the discrimination against $^{13}CO_2$ during CO_2 diffusion through the stomata (4.4‰), *b* — is the
154 discrimination associated with carboxylation (27‰), c_a—ambient CO_2 concentration; $\delta^{13}C_{trc}$—
155 uncorrected $\delta^{13}C$ in tree-ring cellulose data (Farquhar 1989); $\delta^{13}C_a$—data available for $\delta^{13}C$ of
156 atmospheric CO_2 was retrieved from https://www.esrl.noaa.gov/gmd/outreach/isotopes/c13tellsus.html;
157 the 1.6 – is the relationship between water vapor diffusion and CO_2 in the air (Ehleringer and Cerling
158 1995).

159 We used measured CO_2 and $\delta^{13}C$ atmospheric CO_2 data obtained from Manua Loa, Hawaii
160 observations for the recent period (CE 1880-2021) and reconstructed CO_2 and $\delta^{13}C$ of atmospheric
161 CO_2 from ice cores for earlier periods (MacFarling et al., 2006; King et al., 2024; Bauska 2025).

162 Based on the reconstructed CO_2 and the $\delta^{13}C$ of atmospheric CO_2 we computed iWUE in ($\mu mol \cdot mol^{-1}$)
163 for HL and HA regions.

164 ***2.4 Statistical analysis***

165 To distinguish the impact of the two main components as climate and CO_2 concentration we performed
166 correlation analyses between reconstructed iWUE and CO_2 concentration as well as climate variables
167 over the industrial (CE 1900-1998) period.

168 The iWUE chronologies and climate variables for the recent period (since 1900s) were de-trended to
169 avoid coincidence of trends. For de-trending, the linear trend was subtracted from the series (the
170 coefficients of the linear equation were found using the least squares method). Pearson's correlation
171 coefficients between the detrended series were calculated.

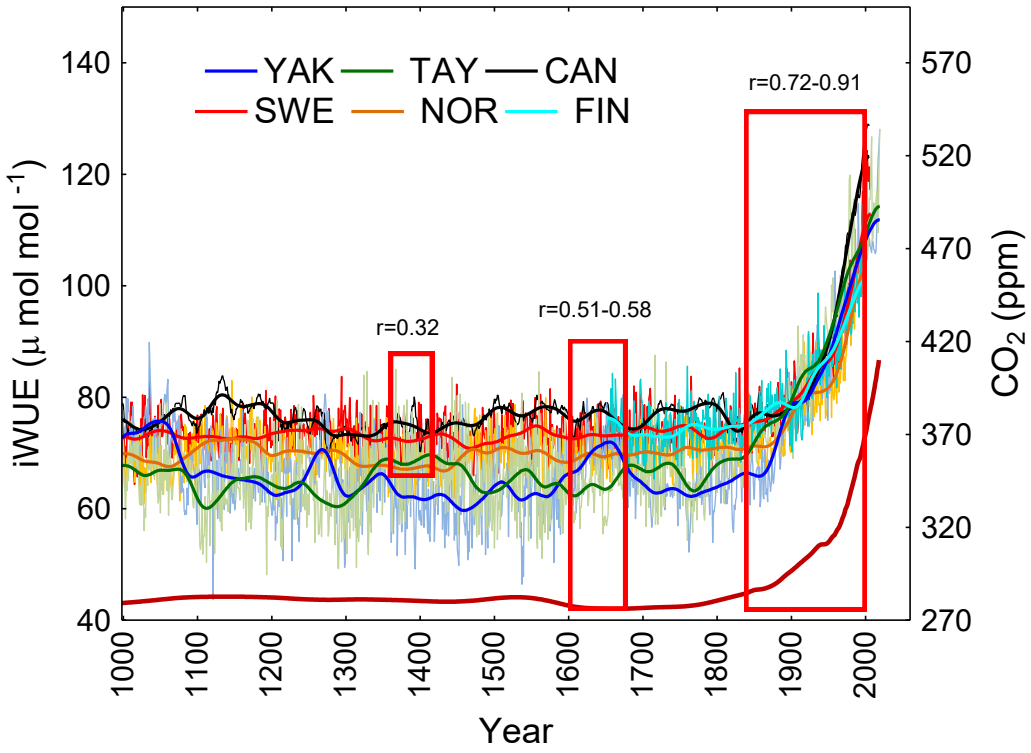
172 **3. Results**

173 ***3.1 Millennial annually resolved iWUE chronologies***

174 ***3.1.1 High latitudes (HL)***

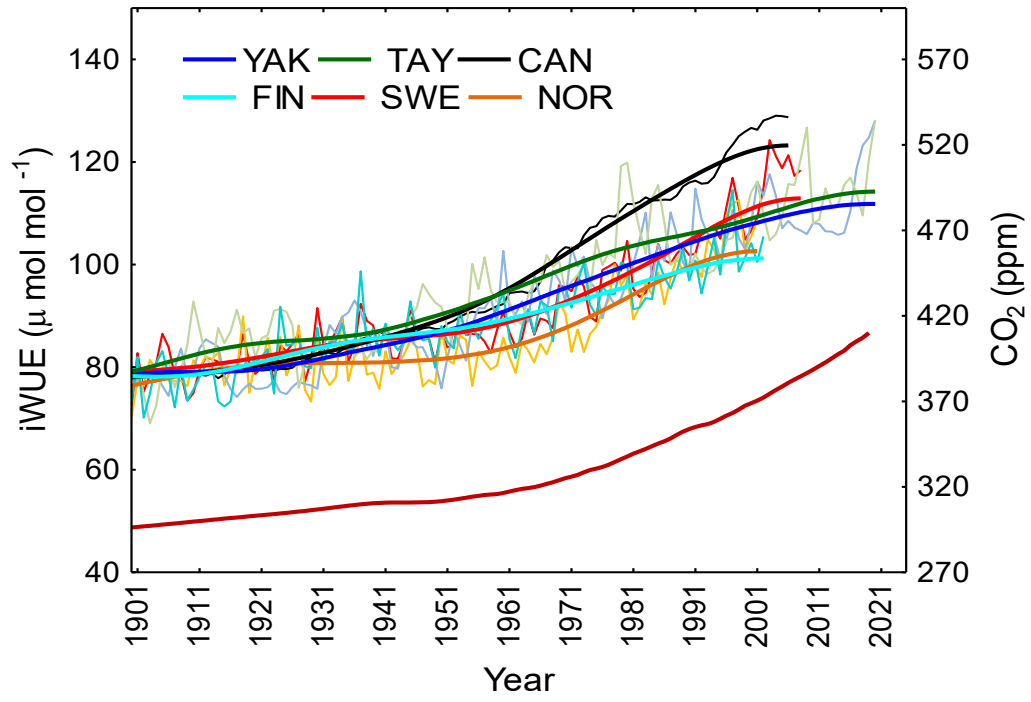
175 Since 1850s the iWUE trends for all studying sites have been steadily increasing and reaching their
176 maximum in 1990s (**Fig.2a, Fig. S2, Table S2**). After 1990s, iWUE trends from Siberian regions
177 (YAK, TAY) demonstrate a plateau effect (**Fig. 2b**). During pre-industrial times, iWUE values were
178 relatively constant with few common patterns for CE 1000-1200 for SWE and NOR sites and for CE
179 1601-1700 for NOR, FIN, SWE, and YAK (**Table S2**). Significant decreases in the ratio of
180 intercellular (c_i) to ambient (c_a) CO_2 concentrations were found for all regions until 2000 (**Fig. 2c, Fig.**
181 **S2**). However, after 2003 increases in the c_i/c_a ratios for SWE, YAK and TAY were detected (**Fig. 2d**).
182 The iWUE for both YAK and TAY show a decrease after 2003 for YAK and after 2009 for TAY with
183 the follow up increase towards 2020 (**Fig. 2d**). Calculated iWUE for conifers along the HL continental
184 gradient derived from $\delta^{13}C$ in tree-ring cellulose clearly show an increase *ci/ca* ratio by coniferous
185 trees that is aligned with the CO_2 increase (**Table 2**). The highest increases in iWUE values were
186 found for trees growing at the most continental sites, that are the sites in Canada, in the eastern part of
187 the Taimyr Peninsula and in northeastern Yakutia. While in the western part of the HL transect iWUE
188 chronologies from FIN and SWE show similar patterns, except for the time span between the 1920s
189 and 1950s, where iWUE of pine in Lapland (pink line) increase compared to other western areas and
190 was comparable to the iWUE dynamics in the eastern Taimyr (red line).

191 **(a)**



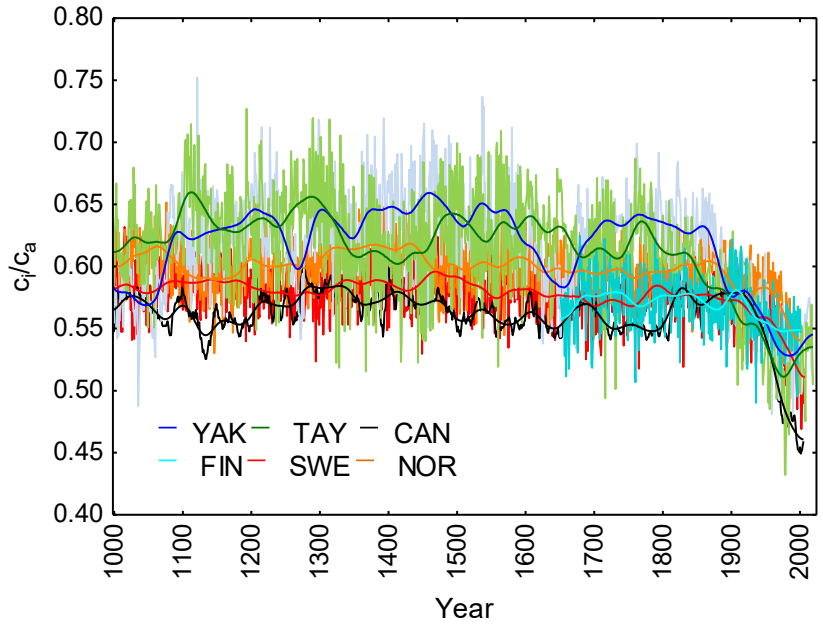
192

193 **(b)**



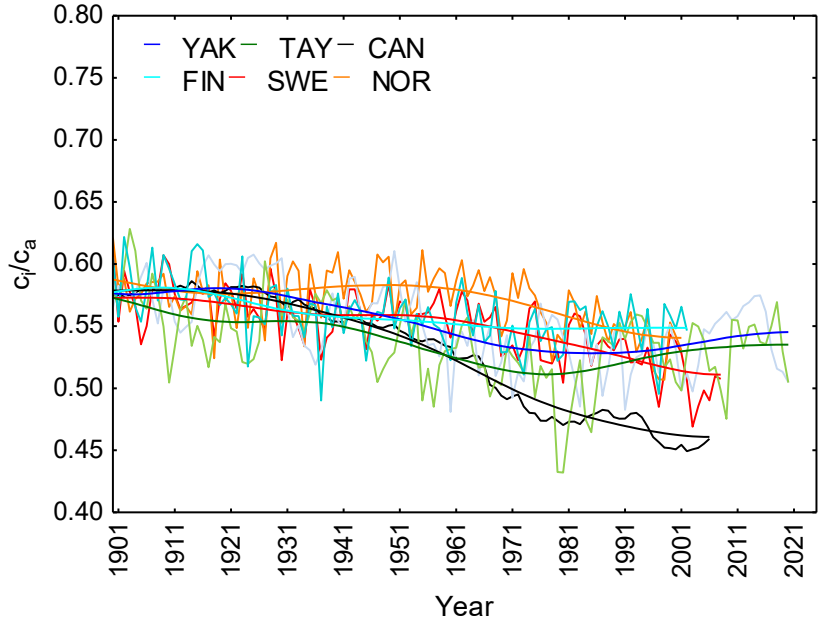
194

195 **(c)**



196

197 **(d)**



198

199 **Figure 2** Annually resolved and smoothed by a 51-year Hamming window reconstructed intrinsic water-
200 use efficiency (iWUE) (**a,b**) and c_i/c_a ratio chronologies (**c,d**) of coniferous trees derived from $\delta^{13}C$
201 values at high-latitude (HL) sites: northeastern Yakutia (YAK, blue line), eastern Taimyr (TAY, green
202 line), Canada (CAN, black line), Laanila (FIN, Finland, light-blue line), Torneträsk (SWE, red line), and
203 Forfojord (NOR, orange line) for the past millennium and the past century. The red boxes highlight

204 significant correlation coefficients between the iWUE time series to illustrate common patterns across
205 different locations (Table S2).

206 **Table 2** The averaged (mean, μmol·mol^{-1}), standard deviation (SD), maximum (max, μmol·mol^{-1}) and
207 minimum (min, μmol·mol^{-1}) intrinsic water-use efficiency (iWUE) values for the last millennium (CE
208 1000-1998) and iWUE differences (diff, %) between pre-industrial (CE 1000-1899) and industrial (CE
209 1900-1998) periods for high-latitude (HL) and high-altitude (HA) sites.

	High-latitude (HL)						**High-altitude (HA)**		
1000-1998	**YAK**	**TAY**	**CAN**	**SWE**	**NOR**	**FIN**	**ALT**	**LOT**	**PAK**
Mean	68.0	68.6	77.9	75.0	71.4	78.6	90.9	78.4	127.8
SD	9.8	10.4	7.0	6.4	6.5	8.2	10.3	7.6	7.4
Max	114.8	119.8	125.0	116.9	112.6	114.5	145.7	122.0	168.2
Min	43.7	48.2	69.7	63.9	59.7	64.8	67.9	65.0	113.9
1000-1899									
Mean	65.7	66.0	76.3	73.5	69.8	75.0	88.4	76.6	126.1
SD	6.4	6.4	2.3	3.4	3.8	4.1	6.3	4.2	3.7
Max	89.9	87.6	83.8	85.3	83.0	88.4	107.1	92.8	141.8
Min	43.7	48.6	69.7	63.9	59.7	64.8	68.0	65.0	113.9
1900-1998									
Mean	88.9	92.1	93.1	88.9	85.4	87.8	113.8	94.9	144.1
SD	10.5	10.2	14.0	9.3	8.9	8.6	11.8	11.0	11.8
Max	114.8	119.9	125.0	116.9	112.6	114.5	145.7	122.0	168.2
Min	74.2	69.0	77.8	71.9	70.1	70.2	89.4	78.4	124.7
Diff, %	**30.1**	**33.0**	**19.8**	**18.9**	**20.1**	**15.7**	**25.1**	**21.3**	**13.3**

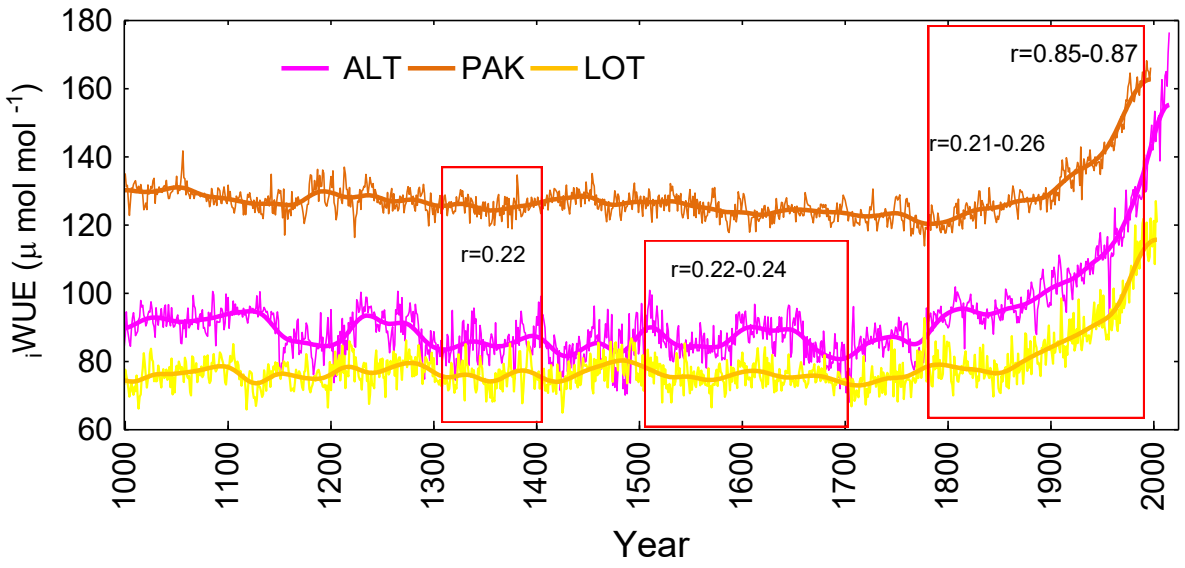
210

The mean iWUE varies for the common period (CE 1000-1998) across HL gradient from 68.0 µmol·mol^{-1} for YAK to 78.6 µmol·mol^{-1} for FIN (**Table 2**). Maximum values for all HL chronologies were found mainly for the recent period (CE 1900-1998) (**Table 2a**). The largest difference between the pre-industrial (CE 1000-1899) and industrial period (CE 1900-1998) was found across HL for TAY (33.0 %) compared to the lowest value for FIN (15.7%) (**Table 2**).

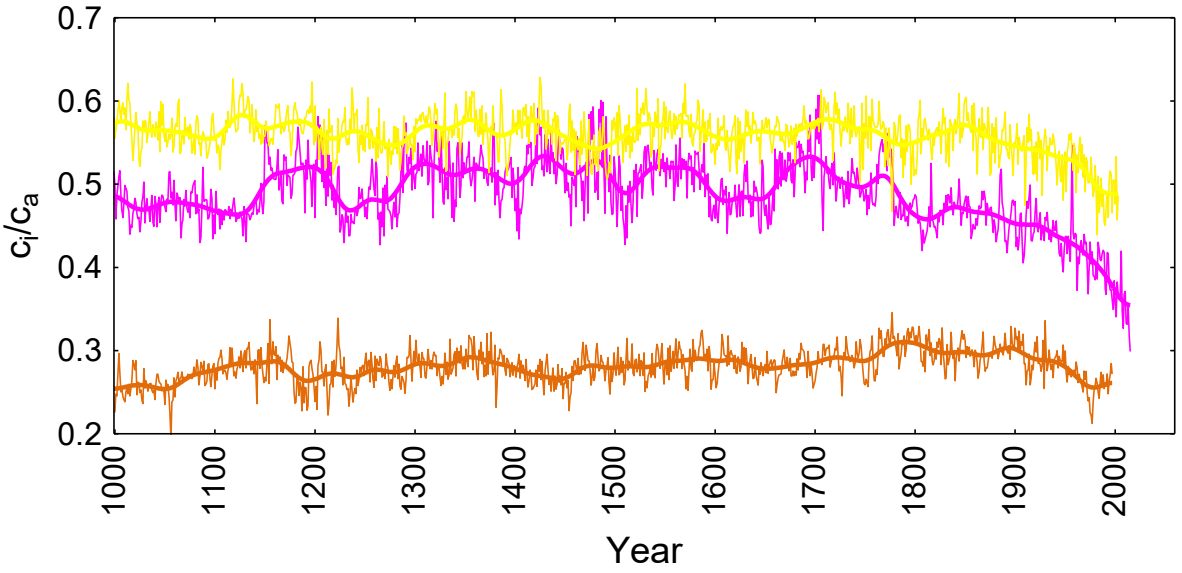
High altitudes (HA)

The millennial iWUE reconstructions show moderate variations during pre-industrial time, with a slight overall decrease towards 1800s for PAK (**Fig. 3a**).

a)



227 **b)**



228

229 **Figure 3.** Annually resolved reconstructed and smoothed by a 51-year millennial iWUE (**a**) and the
230 changes of the c_i/c_a ratio (**b**) from the Altai (ALT), Pakistan, Moor (PAK) and the Loetschental (LOT)
231 for the past millennium (CE 1000-1998). The red boxes highlight significant correlation coefficients
232 between the iWUE time series to illustrate common patterns across different locations (Table S2).

233

234 The increase in iWUE values from CE 1801 towards 1989 is observed for ALT, LOT and PAK (**Fig. 3a,**
235 **Fig S3**), which is confirmed by significant trends and correlations ranges (r = 0.21-0.87, *P<0.01*)
236 between iWUE chronologies (**Table S3**). Similar fluctuations between ALT and LOT were found for
237 CE 1501-1700, while for LOT and PAK for CE 1301-1400.

238 The iWUE values for juniper trees from PAK are generally higher than any of the HA sites, which are
239 covered by larch trees (**Fig. 3b**). Significant increasing trends for iWUE are observed after 1900s, with
240 increasing CO_2 in the atmosphere. Towards the end of the records only ALT shows a continuous
241 increasing iWUE, while for LOT and PAK sites a slow-down of the increase and the beginning of a
242 plateau is observed (**Fig. 3b**).

The HA c_i/c_a for all chronologies (**Fig. 3b, Fig. S3**) show pronounced decrease in response to increasing CO_2. A decrease in the c_i/c_a ratio (**Fig. 3b, Fig. S3**) is found for ALT and LOT, which are represented by larch trees compared to juniper trees in PAK. Relatively constant c_i/c_a values with a slight decrease after 1960s are observed for PAK.

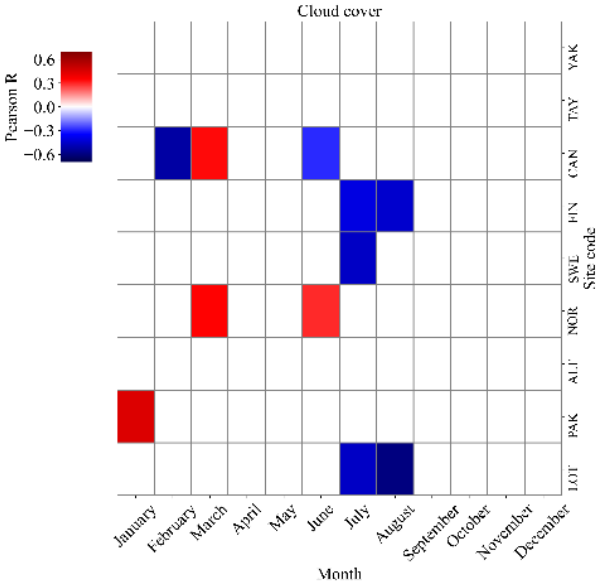
The mean iWUE values vary from 78.4 $\mu mol \cdot mol^{-1}$ for LOT to 127.8 $\mu mol \cdot mol^{-1}$ for PAK over the last millennium (CE 1000-1998) (**Table 2**). The difference between past millennia (CE 1000-1899) and recent period (CE 1900-1998) was found for ALT (25.1 %), less for both LOT (21.3 %) and PAK (13.3 %) (**Table 2**). Sites with relatively high continentality display also a relatively strong increase in iWUE both for HL and HA.

3.2 Influence of CO_2 and climate on iWUE

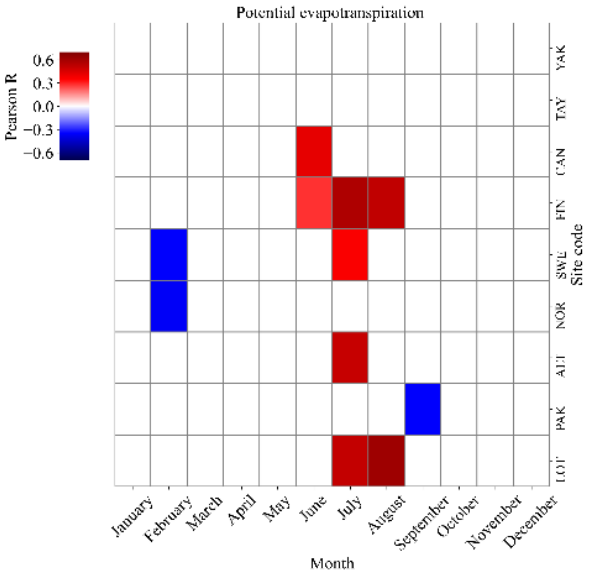
Results of the correlation analysis between de-trended iWUE and monthly gridded climate data such as cloud cover, potential evapotranspiration, precipitation, air temperature, relative humidity and vapor pressure deficit across HL and HA sites show significant ($P<0.01$) correlations over the industrial period (**Fig. 4, Table S4**). Negative significant correlations between iWUE and summer cloud cover were found mainly for western sites like CAN, FIN, SWE, and less for the continental LOT site; while a positive significant correlation was found for NOR (**Fig. 4a**). Significant correlations were found also between summer potential evapotranspiration and iWUE for CAN, FIN, SWE and ALT, LOT, while negative correlation was detected for PAK (**Fig. 4b**). Negative significant correlations with summer (July, or July-August) precipitation were found for TAY, FIN at HL as well as for ALT and LOT from HA (**Fig. 4c, Table S4c**).

The most consistent signal across all sites was found for summer air temperature (**Fig. 4d**). Summer relative humidity (**Fig. 4e**) and precipitation (**Fig. 4c**) show negative correlations with TAY, SWE, ALT and PAK, while positive with PAK. Positive significant correlations between summer VPD and iWUE from the HL: YAK, TAY, CAN, FIN and the HA: ALT, LOT. While negative correlation between iWUE from PAK and summer-autumn VPD were revealed (**Fig. 4d**).

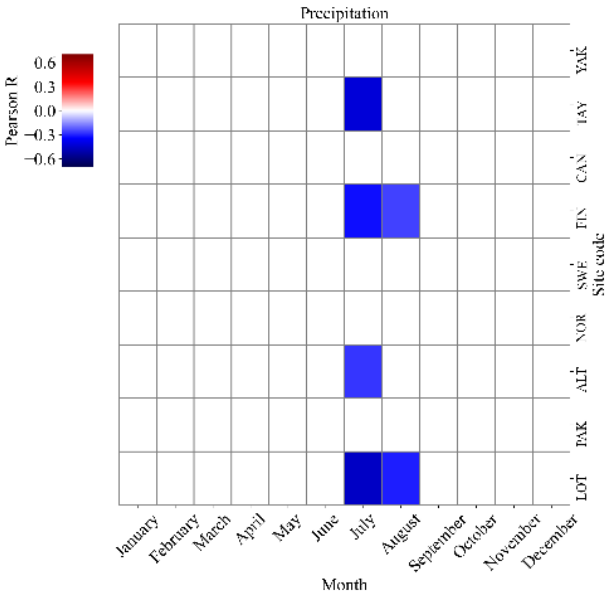
(a) Cloud cover



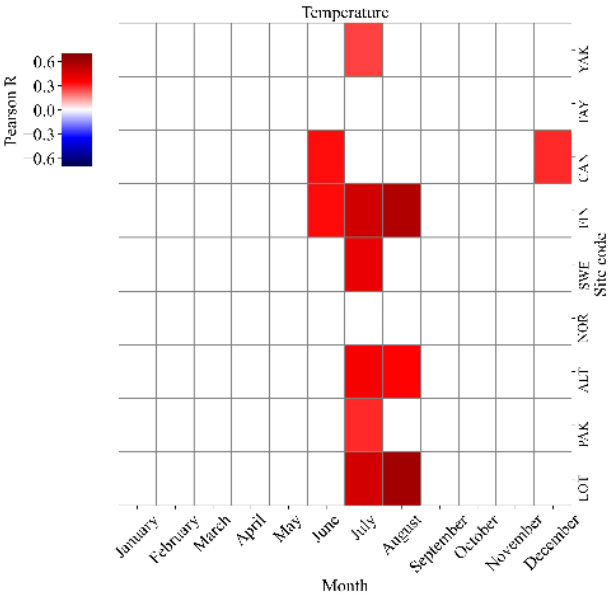
(b) Potential evapotranspiration



(**c**) Precipitation



(d) Air temperature



(e) Relative humidity

(**f**) Vapor Pressure Deficit

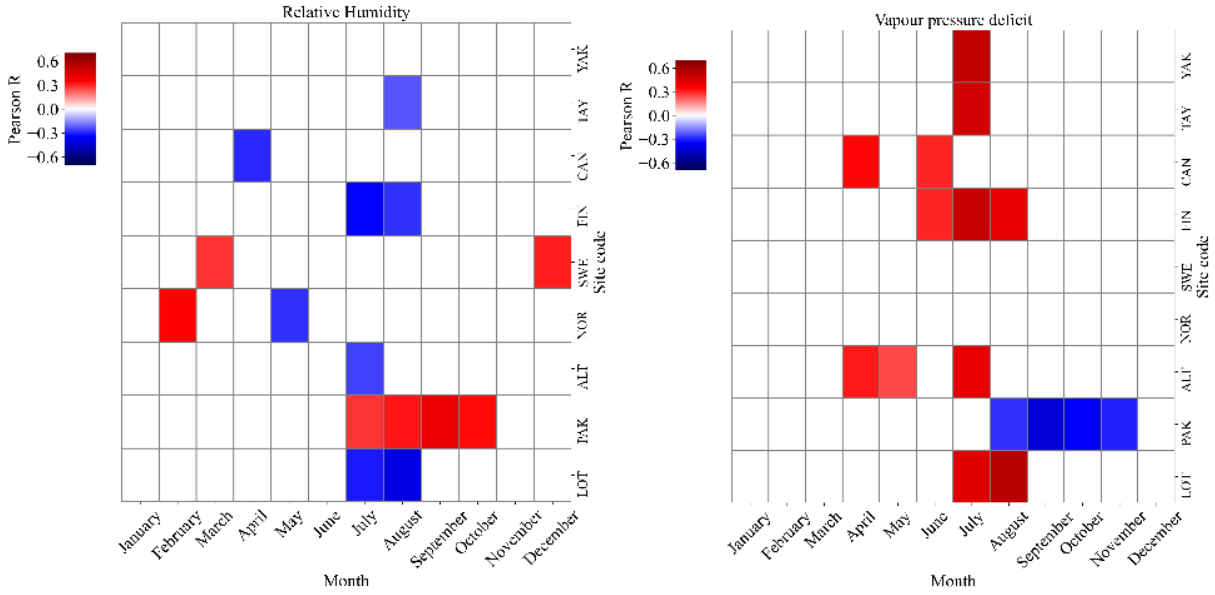
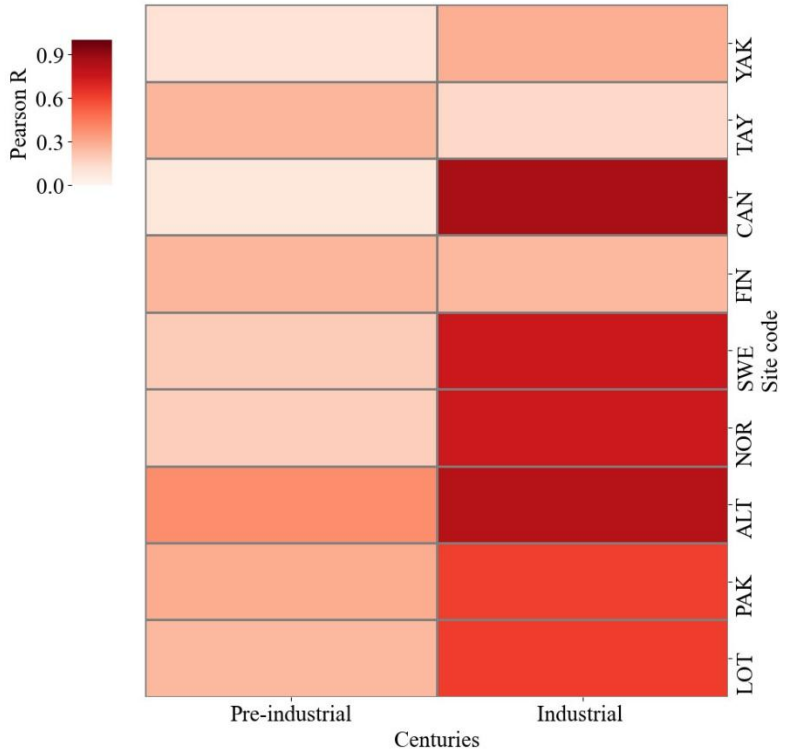


Figure 4. Significant correlation coefficients only (*P<0.01*) between de-trended iWUE and climate variables: cloud cover (**a**), potential evapotranspiration (**b**), precipitation (**c**), air temperature (**d**), relative humidity (**e**) and vapor pressure deficit (**f**) computed for all study sites. Pearson correlations are represented from a negative (-0.6 in a blue colour) to a positive (+0.6 in a dark red colour) value.

Comparing de-trended iWUE and CO_2 concentration for the industrial (CE 1900-1998) period, we found highly significant correlations for all sites (r=0.9, *P<0.001*) (**Fig. 5, Table S5**), with lower values for YAK, TAY and FIN compared to other sites. However, correlation coefficients for the pre-industrial (CE 1000-1899) period are less pronounced compared to the industrial (CE 1900-1998) ones.



284

285 **Figure 5.** Pearson correlation coefficients were found between de-trended intrinsic water use
286 efficiency iWUE versus CO_2 concentration over the pre-industrial (CE 1000-1899) and industrial (CE
287 1900-1998) periods. Significant *P-values <0.001* level are presented from 0.3-0.9 between light to
288 dark red colour.

289

290 Higher correlations between de-trended iWUE and CO_2 for the central TAY and western (FIN, SWE,
291 NOR) parts of subarctic, as well as Inner- and High- Asian sites were found for the pre-industrial
292 period. It is important to highlight that northeastern YAK and CAN sites are showing the smallest
293 impact of CO_2 over the CE 1000-1899 compared to the CE 1900-1998. The most significant impact of
294 CO_2 is detected for CAN over the industrial period.

295 **4. Discussion**

296 ***4.1 Forest water-use strategies at HL and HA regions***

297 We observed increasing iWUE in the industrial period at all sites, but to a different degree. The more
298 pronounced iWUE trend in the northeastern compared to the western part of the subarctic could be
299 explained by the increasing water availability towards the North Atlantic Ocean. While for high-
300 elevated sites with increasing elevation from 2100 to 2900 m asl drought is also increasing jointly with
301 a stronger iWUE response to CO_2. By the common pathway through stomatal pores, the interaction of
302 water availability with CO_2 effects on photosynthesis is expected to be important in evaluating iWUE.
303 The presence of permafrost and its melting during the summer period plays an important role as a
304 reservoir for an additional source of water during dry and hot summers, which can be utilized by
305 conifer trees. This can ameliorate drought stress and lead to adaptation strategies under enhanced air
306 temperature or a significant reduction of precipitation. In contrast, there is a lack of permafrost at the
307 PAK and LOT sites, where trees can be exposed more strongly to drought stress due to a significant
308 reduction of precipitation. Our results suggest that juniper trees from PAK are better adapted to the
309 recent climatic changes, as they were mostly exposed to repeated severe drought stress with only
310 periodic monsoonal water supplies for the past millennia (Treydte et al., 2006). In contrast, larch trees
311 in the Swiss Alps (LOT) were also sensitive to drought conditions (Kress et al., 2010) whereas the
312 water supply via precipitation was lower for the recent decades. Therefore, it is expected that these
313 trees will reduce their stomatal conductance if precipitation levels decline in the future.

314 In ALT the availability of thawed permafrost helps trees to survive drought waves. However, it can
315 become critical if trees do not have access to thawed permafrost water due to limited rooting depth or
316 early snow melt (Churakova (Sidorova) et al., 2020).

317 Numerous studies demonstrated that recent increases in forest water-use efficiency are largely
318 attributable to rising atmospheric CO_2 concentrations, though the magnitude varies by ecosystem and
319 is often moderated by environmental factors (Saurer et al., 2014; Frank et al. 2015; Saurer and Voelker
320 2022; Zhang et al. 2025). Saurer et al. (2014) provided strong long-term evidence that the iWUE of
321 trees has generally increased over the last century, with rising CO_2 concentrations as a major cause, ca.
322 75% of European forests, while growth results depend on drought, nutrients and the local climate. As

323 CO_2 levels rise, the stomata may close partially, thereby maintaining or improving carbon uptake
324 (Saurer and Voelker 2022).

325 As a follow-up study conducted by Frank et al. in 2015 showed, European forests became significantly
326 more water efficient, as a result of rising CO_2 concentration; however, global warming likely prevented
327 a reduction in overall transpiration rates. Site-specific differences, e.g., permafrost availability in the
328 Siberian subarctic (Sidorova et al. 2010) and western Canada (Genaretti et al., 2013), impact of North
329 Atlantic Oscillation on the Fennoscandian sites (Young et al., 2010, 2019) or monsoons in High Asia
330 (Treydte et al. 2006) leave their specific fingerprints in the isotopic patterns. The effects of climate,
331 water and nutrient availability are only modulated by elevated CO_2, but the climate driven response
332 function on iWUE itself does not change.

333 In the pre-industrial period, changes in iWUE have been hardly assessed so far, although there are also
334 significant changes in atmospheric CO_2-concentrations. Observation of a decrease in CO_2
335 concentrations during the 16th and 17th centuries were derived from Law Dome ice core CO_2 records
336 (MacFarling et al., 2006) and West Antarctic Ice Sheet (WAIS) Divide (Bauska et al., 2015), as well as
337 the CO_2 record from Skytrain shows simultaneous decrease in 1610 CE. Common decrease of iWUE
338 values for SWE, NOR, FIN, and YAK for the period from 1601 to 1700 were observed, while
339 increasing iWUE values were mainly revealed towards the modern period CE 1850-1989 (**Table S2,**
340 **3**). But very clearly, the industrial iWUE increase is unprecedent for both HL and HA regions over the
341 past millennium. Since 1990s northeastern and eastern Siberian larch forests reached CO_2 saturation,
342 possibly showing an adaptation or limitation to elevated carbon dioxide concentration, compared to
343 western part of subarctic and high elevated sites.

344 Juniper trees from the dry PAK site do not show such a drastic iWUE increase towards 20th century as
345 the trees at ALT and LOT. Yet, the iWUE values from PAK for the pre-industrial period (between the
346 10th and the beginning of the 19th century) are considerably higher than those from LOT and ALT (**Fig.**

347 **3b**), due to primary dry conditions, indicating on a higher junipers' drought resistance in response to
348 elevated CO_2 and air temperature increase.

349 ***4.2 Potential future iWUE strategies***

350 In a study Ehleringer and Cerling (1995) hypothesized that the level of c_i/c_a under elevated CO_2
351 concentrations will remain constant in most species and although they can vary in others (see also
352 Saurer et al., 2004). For instance, Frank et al., (2015) found that for the industrial period iWUE in
353 broadleaf trees the increase of 14 ± 10 % was less compared to the increase of 22 ± 6% in conifers
354 from European forests along with CO_2 changes, reflecting a clear difference in the ci/ca response
355 during the 20th century. Our study shows a ± 10 % higher change in iWUE for the industrial period
356 (CE 1900-1989) for conifer trees from the subarctic regions, while for high-elevated sites there is a
357 similar range in response to elevated CO_2 (except for PAK). Weiwei et al. (2018) showed that *P.*
358 *orientalis* in semi-arid areas an increased iWUE results from elevated CO_2 concentrations, opposite to
359 other sites e.g., the Swiss Alps (Streit et al., 2014; Churakova (Sidorova) et al., 2016b).
360 A reduced intrinsic water use efficiency response to increasing atmospheric CO_2 concentrations in
361 recent decades was observed primarily at the HL sites. This reduction suggests that more pronounced
362 responses may occur in the future.
363 A further reduction in precipitation, combined with increased temperature resulting from elevated CO_2
364 concentrations and enhanced vapor pressure deficit (VPD), is expected to cause water shortages and
365 drought. This process may initially be reflected in an increase in intrinsic water-use efficiency (iWUE)
366 prior to tree mortality.
367 According to the climate–carbon-cycle model MAGICC7.0 (Meinshausen et al., 2020) the different
368 shared socio-economic pathways scenarios predict a possible future CO_2 concentration increase in the
369 atmosphere by 2100 range from 393 ppm for the lowest (SSP1-1.9) to 1135 ppm for highest (SSP5-
370 8.5) emission scenarios, respectively. According to predicted scenarios it is expected: 1) iWUE is
371 further increasing along with CO_2 towards 2100 or 2) a «plateau effect» with low changes in the c_i/c_a
372 ratio, due to a CO_2 saturation of photosynthesis; or 3) an abrupt iWUE decrease, caused by a faster

reduction of photosynthesis compared to stomatal conductance, e.g., hydraulic failure, leading to drought-induced tree mortality (Arend et al., 2021).

Our findings show that the recent intrinsic water use efficiency (iWUE) pattern at the most continental YAK site aligns with the second and third scenarios, which project a plateau effect and a subsequent decrease through 2100.

The iWUE values in western Fennoscandia are projected to increase twofold in response to a doubling of the global atmospheric CO_2 concentrations. However, current observations indicate that this effect is less pronounced in the region.

Siberian subarctic forests at HL may exhibit adaptive intrinsic water-use efficiency (iWUE) strategies in response to supplementary water from increased thawing of permafrost. In contrast, the western subarctic lacks permafrost and therefore does not benefit from such additional water resources.

5. Conclusion

Our study provides new retrospective insights into forest water-use strategies and survival potential during significant permafrost thaw in northeastern and central regions. We observed increases in iWUE of up to 33.0% at high latitudes and up to 25.1% at three high-elevation sites, likely enhancing forests' influence on regional and global water balances.

We revealed:

1. Despite the strong impact of CO_2 on forest iWUE relative to the pre-industrial (CE 1000-1899) period, the response patterns resulting from climatic variabilities are maintained.

2. Since the 1900s, iWUE changes for the industrial period at the HL and HA are unprecedented over the past millennium. Initially, this is most likely the result of increasing atmospheric CO_2 concentrations, which then reflects the changes in climatic parameters such as reduced precipitation, an increase in air temperature, and VPD; and

3. Siberian forests from northeastern YAK and central TAY demonstrate a considerable resilience towards human-induced CO_2 increase after 2000s.

Author Contributions

OC designed the study, drafted manuscript, performed analyses, interpreted data and wrote the manuscript. MS and RS wrote and reviewed the manuscript. MZ performed climate data analysis and visualization of the heatmaps.

Conflicts of Interest

The authors declare no conflicts of interest.

Data Availability Statement

Data will be available in ZENODO research data repository under the Creative Common CC-BY-4.0 license.

References

Adams, M. A. et al. 2020. Diminishing CO_2-driven gains in water-use efficiency of global forests. *Nat. Clim. Change* 10, 466–471.

Arend, M, Link, R.M., Patthey, R., Schuldt, B., Kahmen, A. 2021. Rapid hydraulic collapse as cause of drought-induced mortality in conifers. PNAS. April 12, 2021, 118 (16)e2025251118; https://doi.org/10.1073/pnas.2025251118

Bauska, T. 2025. Ice core records of atmospheric carbon dioxide, Ed(s): Scott Elias, *Encyclopedia of Quaternary Science* (Third edition), Elsevier, 122-137, ISBN 9780443299971, https://doi.org/10.1016/B978-0-323-99931-1.00264-6.

Bauska, T. K. et al. 2015. Links between atmospheric carbon dioxide, the land carbon reservoir and climate over the past millennium. *Nat. Geosci.* 8, 383–387.

Biskaborn, B.K., Smith, S.L., Noetzli, J. *et al.* 2019. Permafrost is warming at a global scale. *Nat Commun* **10**, 264 https://doi.org/10.1038/s41467-018-08240-4

Bowden, W.B. 2010. Climate change in the Arctic-permafrost, thermokarst, and why they matter to the non-arctic world. *Geography compass* https://doi.org/10.1111/j.1749-8198.2010.00390.

Briffa, K.R., Schweingruber, F.H., Jones, P.D., Osborn, T.H., Shiyatov, S.G., Vaganov, E.A. 1998. Reduced sensitivity of recent tree-growth to temperature at high northern latitudes. *Nature*, Volume 391, Issue 6668, pp. 678-682.

Büntgen, U., Urban, O., Krusic, P.J. *et al.* 2021. Recent European drought extremes beyond Common Era background variability. *Nat. Geosci.* **14**, 190–196 https://doi.org/10.1038/s41561-021-00698-0.

Buck, A. L. 1981. New Equations for Computing Vapor Pressure and Enhancement Factor. *Journal of Applied Meteorology*, **20**(12), 1527–1532. https://doi.org/10.1175/1520-0450(1981)020<1527:NEFCVP>2.0.CO_2.

Cable, D.M., Gino, F., & Staats, B. R. 2013. Breaking them in or eliciting their best? Reframing socialization around newcomers' authentic self-expression. *Administrative Science Quarterly*, 58, 1-36. https://doi.org/10.1177/0001839213477098.

Chen, Z., Zhang, Y., Li, Z., Han, S., Wang, X. 2022. Climate change increased the intrinsic water use efficiency of *Larix gmelinii* in permafrost degradation areas, but did not promote its growth. *Agricultural and Forest Meteorology* (320), 108957, ISSN 0168-1923, https://doi.org/10.1016/j.agrformet.2022.108957.

Churakova, O.V., Porter, T.J., Kirdyanov, A.V., Myglan, V.S., Fonti, M.V., Vaganov, E.A. (2022). Stable Isotopes in Tree Rings of Boreal Forests. In: Siegwolf, R.T.W., Brooks, J.R., Roden, J., Saurer, M. (eds) Stable Isotopes in Tree Rings. Tree Physiology, vol 8. Springer, Cham. https://doi.org/10.1007/978-3-030-92698-4_20

Churakova (Sidorova), O.V., Porter, T.J., Zharkov, M.S., Fonti, M.V., Barinov, V.V., Taynik, A.V., Kirdyanov, A.V., Knorre, A.A., Wegmann, M., Trushkina, T.V., Koshurnikova, N.N., Vaganov, E.A., Myglan, V.S., Siegwolf, R.T.W., Saurer, M. 2023. Climate impacts on tree-ring stable isotopes across the Northern Hemispheric boreal zone. *Science of The Total Environment*, Volume 870, 161644, ISSN 0048-9697, https://doi.org/10.1016/j.scitotenv.2023.161644.

Churakova, O. V. *et al.* 2016a. Application of eco-physiological models to the climatic interpretation of $\delta^{13}C$ and $\delta^{18}O$ measured in Siberian larch tree-rings. *Dendrochronologia* **39**, 51–59.

Churakova (Sidorova) O.V., Saurer, M., Bryukhanova, M.V., Siegwolf, R. T.W., Bigler, C. 2016b. Site-specific water-use strategies of mountain pine and larch to cope with recent climate change. *Tree Physiology*, 36(8), 942–953, https://doi.org/10.1093/treephys/tpw060

Churakova (Sidorova), O.V., Fonti, M.V., Siegwolf, R.T.W., Saurer, M., Myglan, V.S. 2020. Impact of recent climate change on water-use efficiency strategies of *Larix sibirica* in the Altai-Sayan Mountain Range. *Forests* 11, no. 10: 1103. https://doi.org/10.3390/f11101103.

Churakova-Sidorova, O.V., Corona, C., Fonti, M.V. *et al.* 2020a. Recent atmospheric drying in Siberia is not unprecedented over the last 1,500 years. *Sci Rep* **10**, 15024. https://doi.org/10.1038/s41598-020-71656-w.

Churakova (Sidorova), O.V., Fonti, M.V., Siegwolf, R.T.W., Saurer, M., Myglan, V.S. 2020b. Impact of Recent Climate Change on Water-Use Efficiency Strategies of *Larix sibirica* in the Altai-Sayan Mountain Range. *Forests*, *11*, 1103. https://doi.org/10.3390/f11101103.

Churakova (Sidorova), O.V., Porter, T.J., Kirdyanov, A.V., Myglan, V.S., Fonti, M.V., Vaganov, E.A. Stable Isotopes in Tree Rings of Boreal Forests. 2022a. In: Siegwolf, R.T.W., Brooks, J.R., Roden, J., Saurer, M. (eds) Stable Isotopes in Tree Rings. *Tree Physiology*, 8. Springer, Cham. https://doi.org/10.1007/978-3-030-92698-4_20.

Churakova-Sidorova, O.V., Myglan, V.S., Fonti, M.V. *et al.* 2022b. Modern aridity in the Altai-Sayan Mountain range derived from multiple millennial proxies. *Sci Rep* **12**, 7752. https://doi.org/10.1038/s41598-022-112929-1.

Druckenmiller, M. L., Thoman, R. L., Moon, T. A. 2025. NOAA technical report OAR Arctic Report Card; 25-01 (Arctic Report Card) DOI: https://doi.org/10.25923/nrzf-j897

Ehleringer, J.R., Cerling, T.E. 1995. Atmospheric CO_2 and the ratio of intercellular to ambient CO_2 concentrations in plants. *Tree Physiology* 15, 105. Heron Publishing, Victoria, Canada.

Farquhar, G.D., Ehleringer, I.J.R., Hubick, K.T. 1989. Carbon isotope discrimination and photosynthesis. *Annual Review of Plant Biology* **40**: 503–537.

Frank, D.C., Poulter, B., Saurer, M., Esper, J., Huntingford, C., Helle, G., Treydte, K., Zimmermann, N.E., Schleser, G.H., Ahlström, A. *et al*. 2015. Water-use efficiency and transpiration across European forests during the Anthropocene. *Nature Climate Change* **5**: 579–583, DOI: 10.1038/NCLIMATE2614

Gagen, M. *et al*. 2011. Evidence of changing intrinsic water-use efficiency under rising atmospheric CO_2 concentrations in Boreal Fennoscandia from subfossil leaves and tree ring delta ^{13}C ratios. *Global Change Biology* 17, 1064–1072, https://doi.org/10.1111/j.1365-2486.2010.02273.x.

Gennaretti, F., Arseneault, D., Nicault, A., Perreault, L., Bégin, Y. 2014. Volcano-induced regime shifts in millennial tree-ring chronologies from northeastern North America. Proc Natl Aca Sci, USA 111:10077-10082, https://doi.org/10.1073/pnas.1324220111

Gennaretti, F., Huard, D., Naulier, M. *et al. 2017.* Bayesian multiproxy temperature reconstruction with black spruce ring widths and stable isotopes from the northern Quebec taiga. *Clim Dyn* **49**, 4107–4119. https://doi.org/10.1007/s00382-017-3565-5

Gessler, A., Ferrio, J.P. 2022. Chapter 13: Post photosynthetic fractionation in leaves, phloem and stem. In: RTW Siegwolf, JR Brooks, J Roden, M Saurer, eds. *Stable isotopes in tree rings*. Cham, Switzerland: Springer, 381–396.

Guerrieri, R., Belmecheri, S., Ollinger, S.V., Asbjornsen, H., Jennings, K., Xiao, J., Stocker, B.D., Martin, M., Hollinger, D.Y., Bracho-Garrillo, R. *et al*. 2019. Disentangling the role of photosynthesis and stomatal conductance on rising forest water-use efficiency. *Proceedings of the National Academy of Sciences, USA* **116**: 16909–16914.

Helama, S., Arppe, L., Timmonen, M., Mielikäninen, K., Oinonen, M. 2018. A 7.5 ka chronology of stable carbon isotopes from tree rings with implications for their use in palaeo-cloud reconstruction. *Global and Planetary Changes* **170**: 20-33 https://doi.org/10.1016/j.gloplacha.2018.08.002

Climate Change IPCC 2007: Synthesis Report. Contribution of Working Groups I, II and III to the Fourth Assessment Report of the Intergovernmental Panel on Climate Change [Core Writing Team, Pachauri, R.K and Reisinger, A. (eds.)]. IPCC, Geneva, Switzerland, 104 pp.

Jackson, R., Sala, O., Field, C. & Mooney, H. 1994. CO_2 alters water use, carbon gain, and yield for the dominant species in a natural grassland. *Oecologia* **98**, 257–262.

Keeling, C.D., Bacastow, R.B., Bainbridge, A.E., Ekdahl, C.A., Guenther, P.R., Waterman, L.S., 1976. Atmospheric carbon dioxide variations at Mauna Loa Observatory, Hawaii, *Tellus* **28**: 538-551

Keller, K. M., Lienert, S., Bozbiyik, A., Stocker, T. F., Churakova (Sidorova), O. V., Frank, D. C., Klesse, S., Koven, C. D., Leuenberger, M., Riley, W. J., Saurer, M., Siegwolf, R., Weigt, R. B., and Joos, F. 2017. 20th century changes in carbon isotopes and water-use efficiency: tree-ring-based evaluation of the CLM4.5 and LPX-Bern models, *Biogeosciences*, **14**, 2641–2673, https://doi.org/10.5194/bg-14-2641-2017.

King, A.C.F., Bauska, T.K., Brook, E.J. *et al.* 2024. Reconciling ice core CO_2 and land-use change following New World-Old World contact. *Nat Commun* **15**, 1735. https://doi.org/10.1038/s41467-024-45894-9

Körner, C. 2012. Alpine treelines Functional ecology of the global high elevation tree limits, Springer Science & Business Media, 220 p.

513 Kress, A., M. Saurer, R. T. W. Siegwolf, D. C. Frank, J. Esper, H., Bugmann. 2010. A 350-year drought
514 reconstruction from Alpine tree ring stable isotopes, *Global Biogeochem. Cycles* **24**, GB2011,
515 doi:10.1029/2009GB003613

516 Lan, X., NOAA/GML (gml.noaa.gov/ccgg/trends/) R., Keeling, Scripps Institution of Oceanography
517 (scrippsco2.ucsd.edu/).

518 Lan, X., K.W. Thoning, and E.J. Dlugokencky. 2025. Trends in globally-averaged CH_4, N_2O, and SF_6
519 determined from NOAA Global Monitoring Laboratory measurements. Version 2025-03,
520 https://doi.org/10.15138/P8XG-AA10 Trends in CH_4 - NOAA Global Monitoring Laboratory

521 Lavergne, A., Graven, H., De Kauwe, M.G., Keenan, T.F., Medlyn, B.E., Prentice, I.C. 2019. Observed
522 and modelled historical trends in the water-use efficiency of plants and ecosystems. *Global Change*
523 *Biology* **25**: 2242–2257.

524 Lloyd, A.H., Bunn, A.G. 2007. Responses of the Circumpolar Boreal Forest to 20th Century Climate
525 Variability. *Environmental Research Letters* **2**, https://doi.org/10.1088/1748-9326/2/4/045013

526 Loader N.J., Young G.H.F., Grudd H., McCarroll D. 2013. Stable carbon isotopes from Torneträsk,
527 northern Sweden provide a millennial length reconstruction of summer sunshine and its relationship to
528 Arctic circulation, *Quaternary Science Reviews* **62**, 97-113, ISSN 0277-3791,
529 https://doi.org/10.1016/j.quascirev.2012.11.014.

530 MacFarling, M., C., Etheridge, D., Trudinger, C., Steele, P., Langenfelds, R., van Ommen, T., S.A.,
531 Elkins, J. Law. 2006. Dome CO_2, CH_4 and N_2O ice core records extended to 2000 years BP
532 Geographical Research Letter 138 (33), 14, https://doi.org/10.1029/2006GL026152

533 Mathias, J.M., Thomas, R.B. 2021. Global tree intrinsic water use efficiency is enhanced by increased
534 atmospheric CO_2 and modulated by climate and plant functional types. *PNAS* 16: 118(7), 1-9.

McDowell, N., Pockman, W.T., Allen, C.D., Breshears, D.D., Cobb, N., Kolb, T., Plaut, J., Sperry, J., West, A., Williams, D.G., *et al.* 2008. Mechanisms of plant survival and mortality during drought: Why do some plants survive while others succumb to drought? *New Phytol.* **178**, 719–739.

Meinshausen, M., Nicholls, Z. R. J., Lewis, J., Gidden, M. J., Vogel, E., Freund, M., Beyerle, U., Gessner, C., Nauels, A., Bauer, N., Canadell, J. G., Daniel, J. S., John, A., Krummel, P. B., Luderer, G., Meinshausen, N., Montzka, S. A., Rayner, P. J., Reimann, S., Smith, S. J., van den Berg, M., Velders, G. J. M., Vollmer, M. K., and Wang, R. H. J. 2020. The shared socio-economic pathway (SSP) greenhouse gas concentrations and their extensions to 2500, Geosci. Model Dev., 13, 3571–3605, https://doi.org/10.5194/gmd-13-3571-2020.

Saurer, M., Schweingruber, F., Vaganov, E.A., Shiyatov, S.G., Siegwolf, R. 2002. Spatial and temporal oxygen isotope trends at the northern tree-line in Eurasia. *Geophysical Research Letters* **29(9)**: 10.1029/2001GL013739.

Saurer, M., Spahni, R., Frank, D.C. et al. 2014. Spatial variability and temporal trends in water-use efficiency of European forests. *Global Change Biol* **20**, 3700-3712, doi:10.1111/gcb.12717.

Saurer, M., Siegwolf, R.T.W., Schweingruber, F.H. 2004. Carbon isotope discrimination indicates improving water-use efficiency of trees in northern Eurasia over the last 100 years. *Global Change Biology* **10**: 2109–2120.

Saurer, M., Voelker, S. 2022. Intrinsic Water-Use Efficiency Derived from Stable Carbon Isotopes of Tree-Rings. In: Siegwolf, R.T.W., Brooks, J.R., Roden, J., Saurer, M. (eds) Stable Isotopes in Tree Rings. *Tree Physiology* **8**. Springer, Cham. https://doi.org/10.1007/978-3-030-92698-4_17.

Sidorova, O.V., Siegwolf, R., Saurer, M., Shashkin, A.V., Knorre, A.A., Prokushkin, A.S., Vaganov, E.A., Kirdyanov, A.V. 2009. Do centennial tree-ring and stable isotope trends of *Larix gmelinii* (Rupr.) Rupr. indicate increasing water shortage in the Siberian north? *Oecologia*, 10.1007/s00442-009-1411-0, 1432-1939.

559 Sidorova, O.V., Siegwolf, R., Saurer, M., Naurzbaev, M., Shashkin, A.V., Vaganov, E.A. 2010. Spatial
560 patterns of climatic changes in the Eurasian north reflected in Siberian larch tree-ring parameters and
561 stable isotopes. *Global Change Biology* **16**, 1003-1018, 10.1111/j.1365-2486.2009.02008.x.

562 Sidorova, O.V., Saurer, M., Myglan, V.S., Eichler, A., Schwikowski, M., Kirdyanov, A.V.,
563 Bryukhanova, M.V., Gerasimova, O.V., Kalugin, I., Daryin, A., Siegwolf, R. 2012. A multi-proxy
564 approach for revealing recent climatic changes in the Russian Altai. *Climate Dynamics* **38**: (1-2) 175–
565 188.

566 Sidorova, O.V., Siegwolf, R., Saurer, M., Naurzbaev, M.M., Vaganov, E.A. 2008. Isotopic composition
567 ($\delta^{13}C$, $\delta^{18}O$) in Siberian tree-ring chronology. *Geophys. Res. Biogeoscinces* **113**, G02019,
568 doi:10.1029/2007JG000473.

569 Dawson, T.E. and Siegwolf, R.T.W (Ed.) (2007) Stable isotopes as indicators of ecological change.
570 Terrestrial ecology series. London: Academic Press, 417 p.

571 Soja, A.J., Tchebakova, N.M., French, N.H.F., Flannigan, M.D., Shugart, H.H., Stocks, B.J., Sukhinin,
572 A.I., Parfenova, E.I., Chapin, III. F.S., Stackhouse, P.W. Jr. 2007. Climate-induced boreal forest
573 change: Predictions versus current observations, *Global and Planetary Change* **56**, 274-296.

574 Streit, K., Siegwolf, R.T.W., Hagerdon, F, Schaub, M., Buchmann, N. 2014. Lack of photosynthetic or
575 stomatal regulation after 9 years of elevated [CO_2] and 4 years of soil warming in two conifer species
576 at the alpine treeline. *Plant, Cell and Environment* **37**(2), 315-326.

577 Tang, Yu., Sahlstedt, E., Young, G., et al. 2023. Estimating intraseasonal intrinsic water-use efficiency
578 from high-resolution tree-ring $\delta^{13}C$ data in boreal Scots pine forests. *New Phytologist* 237, 1606-1619
579 https://doi.org/10.1111/nph.18649.

580 Treydte, K.S., Schleser, G.H., Helle, G., Frank, D.C., Winiger, M., Haug, G.H., Esper, J. 2006. The
581 twentieth century was the wettest period in northern Pakistan over the past millennium, *Nature*, **440**,
582 27, doi:10.1038/nature04743.

583 Treydte, K., Frank, D.C., Saurer, M., Helle, G., Schleser, G., Esper, J. 2009. Impact of climate and
584 CO_2 on a millennium-long tree-ring carbon isotope record. *Geochimica et Cosmochimica Acta* **73**
585 4635–4647.

586 Turetsky, M.R., Abbott, B.W., Jones, M.C., Anthony, K.W., Olefeldt, D., Schuur, E.A.G., Koven, C.,
587 McGuire, A.D., Grosse, G., Kuhry, P., Hugelius, G., Lawrence, D.M., Gibson, C., Sannel, A.B.K.
588 2019. Permafrost collapse is accelerating carbon release *Nature* **569,** 10.1038/d41586-019-01313-4

589 Vaganov, E.A., Hughes, M.S., Shashkin, A.V. 2006. Growth Dynamics of Conifer Tree Rings

590 358 pp, 10.1007/3-540-31298-6

591 Waskom, M.L. 2021. The Matplotlib Basemap Toolkit 1.4.1.

592 Weiwei, L.U., Xinxiao, Y.U., Guodong, J.I.A. *et al.* 2018. Responses of intrinsic water-use efficiency
593 and tree growth to climate change in semi-arid areas of North China. *Sci Rep* **8,** 308.
594 https://doi.org/10.1038/s41598-017-18694-z.

595 Wang, W, Liu, X., Xu, G., Zeng X., Wu, G, Zhang X, Qin D 2016. Temperature signal instability of
596 tree-ring δ13C chronology in the northeastern Qinghai–Tibetan Plateau, *Global and Planetary*
597 *Change*, **139**, 165-172, ISSN 0921-8181, https://doi.org/10.1016/j.gloplacha.2016.02.006.

598 Williams, A., Allen, C.D., Macalady, A.K., Griffin, D., Woodhouse, C.A., Meko, D.M., Swetnam,
599 T.W., Rauscher, S.A., Seager, R., Grissino-Mayer, H.D., *et al.* 2013. Temperature as a potent driver of
600 regional forest drought stress and tree mortality. *Nat. Clim. Chang,* **3**, 292–297.

601 Weiwei, L.U., Xinxiao, Y.U., Guodong, J.I.A. *et al.* 2018. Responses of Intrinsic Water-use Efficiency
602 and Tree Growth to Climate Change in Semi-Arid Areas of North China. *Sci Rep* **8**, 308.
603 https://doi.org/10.1038/s41598-017-18694-z.

Young, G. H. F., D. McCarroll, N. J. Loader, Kirchhefer, A. 2010. A 500-year record of summer near-ground solar radiation from tree-ring stable carbon isotopes, *The Holocene*, **20**(3), 315–324, doi:10.1177/0959683609351902.

Young, G.H.F., Gagen, M.H., Loader, N.J., McCarroll, D., Grudd, H., Jalkanen, R., Kirchhefer, A., Robertson, I. 2019. Cloud cover feedback moderates Fennoscandian summer temperature changes over the past 1,000 years. *Geoph. Res. Lett.* **46**, 2811-2819, https://doi.org/10.1029/2018GL081046.

Yuan, W., Zheng, Y., Piao, S., Ciais, P., Lombardozzi, D., Wang, Y., Ryu, Y., Chen, G., Dong, W., Hu, Z., *et al.* 2019. Increased atmospheric vapor pressure deficit reduces global vegetation growth. *Sci. Adv.* **5**, eaax1396.

Zandt, M.H., Liebner, S., Welte, C.U. 2020. Roles of thermokarst lakes in a warming world. *Trends in microbiology*, **28**(9), 769-779.

Zhang, Q., Ficklin, D.L., Manzoni, S., Wang, L., Way, D., Phillips, R.P., Novick, K.A. 2019. Response of ecosystem intrinsic water use efficiency and gross primary productivity to rising vapor pressure deficit. *Environ. Res. Lett.*, **14**, 074023.

Zhang, Q., Zhang, J., Adams, M.A. *et al.* 2026 Increased efficiency of water use does not stimulate tree productivity. *Nat. Clim. Chang.* **16**, 87–94, https://doi.org/10.1038/s41558-025-02504-w.

Zharkov, M.S., Fonti, M.V., Trushkina, T.V., Barinov, V.V., Taynik, A.V., Porter, T.J., Saurer, M., Churakova, O.V. 2021. Mixed temperature-moisture signal in $\delta^{18}O$ records of Boreal conifers from the permafrost zone. *Atmosphere*, **12**, 1416. https://doi.org/10.3390/atmos12111416t.

Supplementary Files

This is a list of supplementary files associated with this preprint. Click to download.

- 20260509CEEChurakovaetalSuppMat.docx